Articles

Synthesis, Characterization, and Ion Exchange Behavior of a Framework Potassium Titanium Trisilicate $K_2TiSi_3O_9·H_2O$ and Its Protonated Phases

Anatoly I. Bortun, Lyudmila N. Bortun, Damodara M. Poojary, Ouyang Xiang, and Abraham Clearfield*

Texas A&M University, Chemistry Department, College Station, Texas 77843-3255

Received March 2, 1999. Revised Manuscript Received November 9, 1999

A framework potassium titanium silicate $K_2TiSi_3O_9·H_2O$, compound I, was synthesized by the reaction of a titanium−hydrogen peroxide complex and SiO_2 in alkaline media under mild hydrothermal conditions (180 °C). This compound was converted to the corresponding sodium phase, $Na_2TiSi_3O_9·H_2O$ (IV) and two proton-containing phases, $K_{1.26}H_{0.74}TiSi_3O_9·1.8H_2O$ (II) and $K_{0.3}H_{1.7}TiSi_3O_9·2.4H_2O$ (III) by ion exchange. These products were characterized by elemental analysis, TGA, FT-IR, MAS ^{29}Si NMR, and X-ray diffraction. The ion exchange behavior of $K_2TiSi_3O_9·H_2O$ and $K_{0.3}H_{1.7}TiSi_3O_9·2H_2O$ toward alkali, alkaline earth, and some transition metal ions solutions was studied. A high affinity of the protonic form of titanium trisilicate exchanger for cesium and potassium makes it promising for radionuclide-contaminated groundwater treatment and certain analytical separations. The crystal structure of $K_2TiSi_3O_9·H_2O$ was found to be isomorphous with that of the zirconium analogue and contains a framework enclosing two types of tunnels. The exchange properties were interpreted on the basis of this structure and selectivity of the Zr and Ti phases rationalized on the basis of the tunnel sizes. The structure of II was solved on the basis of a monoclinic cell, whereas the $K_2TiSi_3O_9·H_2O$ phase is orthorhombic. The relationship of structure II, monoclinic, to the parent orthorhombic structure is described. Phase III yielded a complex X-ray pattern with evidence of disorder and a highly complex ^{29}Si NMR spectrum. On reexchanging with K^+, the original crystal lattice was restored.

Introduction

Alkali metal titanium silicates have received considerable attention in recent years.[1−6] This attention is related to the fact that some of them form frameworks that enclose tunnels or pores containing exchangeable ions. Thus, they form members of the ever-expanding family of inorganic ion exchangers.[7−10] Because of their compact structures, they may exhibit prominent selectivity for certain ions, namely, for radiocesium and radiostrontium. Coupled with other valuable properties such as high thermal, chemical and radiation stability, and resistance to oxidation, these compounds are extremely attractive for nuclear waste remediation, ion sieving, and selective separations.

The investigation of alkali metal titanium silicates has shown that a majority of the selective exchangers are crystalline compounds with well-defined three-dimensional framework structures containing zeolite-like tunnels.[2,3,11,12] Recent structural and ion exchange studies have determined that the reason for the unique selectivity of crystalline titanium silicates is related to the correspondence of the geometrical parameters of their ion exchange sites (channels, cavities) to the size of the selectively adsorbed ions.[11−15] Because of the

* To whom correspondence should be addressed.

(1) Kuznicki, S. M. U.S. Patent 4,853,202 **1989**.
(2) Chapman, D. M.; Roe, A. L. *Zeolites* **1990**, *10*, 730.
(3) Kuznicki, S. M.; Trush, K. A.; Allen, F. M.; Levine, S. M.; Hamil, M. M.; Hayhurst, D. T.; Mansour, M. In *Molecular Sieves. Synthesis of Microporous Materials*; Occelli, M. L.; Robson, H., Eds.; Van Nostrand Reinold: New York, NY, 1992; Vol. 1, p 427.
(4) Anthony, R. G.; Philip, C. V.; Dosch, R. G. *Waste Management* **1993**, *13*, 503.
(5) Clearfield, A.; Bortun, A. I.; Bortun, L. N.; Cahill, R. A. *Solvent Extr. Ion Exch.* **1997**, *15*, 285.
(6) Clearfield, A.; Bortun, A. I.; Bortun, L. N. In *Ion Exchange Developments and Applications*; Greig, J. A., Ed.; SCI: Cambridge, 1996; p 338.
(7) *Inorganic Ion Exchange Materials*; Clearfield, A., Ed.; CRC Press: Boca Raton, FL, 1982.
(8) Vesely, V.; Pekarek, V. *Talanta* **1972**, *19*, 219.
(9) *Inorganic Ion Exchangers in Chemical Analysis*; Qureshi, M., Varshney, K. G., Eds.; CRC Press: Boca Raton, FL, 1991.
(10) Clearfield, A. *Ind. Eng. Chem. Res.* **1995**, *34*, 2865.
(11) Poojary, D. M.; Cahill, R. A.; Clearfield, A. *Chem. Mater.* **1994**, *6*, 2364.
(12) Harrison, W. T. A.; Gier, T. E.; Stucky, G. D. *Zeolites* **1995**, *15*, 408.
(13) Bortun, A. I.; Bortun, L. N.; Clearfield, A. *Solvent Extr. Ion Exch.* **1996**, *14*, 341.
(14) Behrens, E. A.; Poojary, D. M.; Clearfield, A. *Chem. Mater.* **1996**, *8*, 1236.
(15) Poojary, D. M.; Bortun, A. I.; Bortun, L. N.; Clearfield, A. *Inorg. Chem.* **1996**, *35*, 6131.

10.1021/cm990126z CCC: $19.00
Published on Web 01/13/2000

small size of the channels or cavities, the framework in a sense acts as a coordinating ligand to the cations. It is therefore of interest to uncover additional novel framework polyvalent metal silicates. In this paper some preliminary results on the synthesis, characterization and ion exchange properties of a new hydrated potassium titanium trisilicate of formula $K_2TiSi_3O_9 \cdot H_2O$ are presented. A zirconium analogue of this compound, having similar structure, was described recently,[16] as was the parent titanium compound,[17] but no ion exchange data was presented for the latter compound.

Experimental Section

Reagents. All reagents were of analytical grade (Aldrich) and used without further purification.

Analytical Procedures. X-ray powder diffraction data for phase identification were collected with a Seifert-Scintag PAD-V diffractometer with Cu Kα radiation. Thermal analysis was performed with a DuPont Instruments TA 4000 unit (under nitrogen, at a heating rate of 10 °C/min). Titanium and silicon content in the solids were determined by using a SpectraSpec Spectrometer DCP-AEC after dissolving a weighed amount of sample in HF. IR spectra were obtained on a Perkin-Elmer 1720-X FT spectrophotometer by the KBr pellet technique. The MAS NMR ^{29}Si spectra were obtained on a Bruker MSL-300 spectrometer at a frequency of 59.6 MHz and at ambient temperature. The spectrometer was equipped with a 7-mm double-resonance magic-angle spinning probe. The radio frequency field strengths for both ^{29}Si and ^{1}H were 62.5 kHz. The magic-angle spinning rate was set to 4200 Hz. The cross-polarization with ^{1}H decoupling experiments were run with a 1.5 ms contact time and a 10-s recycle delay. Experiments with direct ^{29}Si polarization and ^{1}H decoupling used a 45° ^{29}Si pulse with a 20 s recycle delay for acquisition. Spectra were referenced to an external ZSM-5 zeolite sample at −112 ppm as a secondary standard. Electron micrographs were recorded with a JEOL JSM- 6100 electron microscope operating at 20 kV.

Ion Exchange Study. Exchange of alkali and alkaline earth metal cations by the protonated titanium silicate(III) was studied using 0.05 N MCl_n−$M(OH)_n$ (M = Li, Na, K, Cs, Ca, Sr, Ba; n = 1, 2) solutions under batch conditions at V:m = 200:1 (mL:g), room temperature. The ratio of $M(Cl)_n$ to $M(OH)_n$ was varied from 9:1 to 1:9 and the pH measured at equilibrium. Exchange of Co^{2+}, Ni^{2+}, Cu^{2+}, and Cr^{3+} was studied in 0.01−0.1 M solutions with no added base at V:m = 100:1 (mL/g) at room temperature. In all cases the contact time was 5 days with continuous shaking. The pH of solutions after equilibration with the ion exchanger was measured using a Corning-340 pH meter and in the case of the alkali and alkaline earth cations plotted as uptake versus pH. Final concentrations of all the cations in solution were measured using a Varian SpectrAA-300 atomic absorption spectrometer.

Removal of cesium and strontium from groundwater simulant by the proton form of titanium trisilicate(III) was studied by the batch method at V:m ratio 1000:1 (mL/g), ambient temperature and 5 days contact. The groundwater simulant contained Ca, 100 mg/L; Mg, 10 mg/L; Na, 15 mg/L; Sr, 4.6−4.8 mg/L; Cs −5.95 mg/L (pH = 7.5).

The affinity of the titanium silicates to cesium, strontium, and some other elements was expressed through the distribution coefficient (K_d, mL/g) defined as $K_d = (C_o - C_i/C_i) \cdot V/m$, where C_o and C_i are the ion concentrations in the initial solution and in the solution after equilibration with the adsorbent, respectively, and V/m is the volume-to-mass ratio.

Chemical Stability. Stability of the titanium silicate phase to acid and base solutions was determined by a batch technique by contacting 0.1 g of the exchanger with 10 mL of a NaOH or HNO_3 solution of different concentrations for 5 days under ambient temperature. The extent of titanium and silicate release into the solution was determined spectrophotometrically[18] with the use of a UV−vis Perkin-Elmer model 200 instrument.

Synthesis. The hydrated potassium titanium silicate, $K_2TiSi_3O_9 \cdot H_2O$ (I), was prepared as follows: to 30 mL of a 2 M $TiCl_4$ solution, 40 mL of a 30% H_2O_2 solution, 150 mL of distilled water, and 40 mL of a 10 M NaOH solution were added quickly and with stirring. Then 12.6 g of SiO_2 dissolved in 200 mL of a 3 M KOH solution was added to the reaction mixture. The reaction system was treated hydrothermally (180 °C) for 7 days in a 1.0-L Teflon-lined pressure vessel, after which the fine, white dispersed powder was filtered and washed with distilled deionized water and dried at 70−80 °C in air.

Proton-containing forms of the exchanger, $K_{1.26}H_{0.74}Ti(Si_3O_9) \cdot 1.6H_2O$ (II) and $K_{0.3}H_{1.7}TiSi_3O_9 \cdot 2.4H_2O$ (III) were prepared by treatment of the potassium titanium silicate with a 0.5 M acetic acid solution for different lengths of time.

X-ray Data Collection and Structure Refinement. For structure work the X-ray powder data were collected using a flat aluminum sample holder by means of a Rigaku computer-automated diffractometer. The X-ray source was a rotating anode operating at 50 kV and 180 mA with a copper target and graphite-monochromated radiation. Data were collected at room temperature between 10 and 90° and 9.5−85° in 2 θ for compounds I and II, respectively (step size was 0.01° and a count time of 10 s per step). The powder patterns were indexed by Ito methods.[19] The initial unit cell dimensions obtained were as follows: compound I, a = 9.903, b = 12.940, c = 7.136 Å (FOM = 146); compound II, a = 7.222, b = 10.036, c = 12.927 Å, β = 91.445° (FOM = 85). The systematic absences were consistent with the space group $P2_12_12_1$ for compound I and $P2_1/c$ for compound II. Structure factor amplitudes were extracted from the observed X-ray patterns by the LeBail method.[20,21]

The atomic positions for the metal trisilicate group found for the zirconium analogue[16] were used as a starting model for the structure solution of compound I. After initial refinements of the structure and profile functions, difference Fourier maps were computed which allowed the location of the two potassium ions and the water oxygen positions. The full structure was then refined with soft constraints for the silicate groups. In the final stages of refinement the weights of these constraints were reduced and kept at a value sufficient to maintain a satisfactory geometry for the trisilicate group. The preferred orientation factor was refined to a value very close to 1.0. The diffraction vector is along the c* axis and the ratio of the effect along this axis to that along the perpendicular plane was refined. All the atoms were refined isotropically. Neutral atomic scattering factors, as stored in GSAS,[20] were used for all atoms. No corrections were made for absorption.

Compound II crystallizes in a different Laue symmetry than compound I but their structures are related. The unit cell dimensions, a, b, and c in I correspond to b, c, and a in compound II. In addition, the monoclinic angle, β [91.447(1)°] is close to 90°. On the basis of this relationship, the structural model for the metal silicate group obtained for compound I was transformed to the unit cell of compound II. To define the structure with respect to the right origin in the space group $P2_1/c$, it was necessary to transform the coordinates as follows: $X_m = Z_o$, $Y_m = {}^1/_4 + X_o$, $Z_m = Y_o$ where subscript m represents monoclinic and o orthorhombic. This new model gave a satisfactory fit with the observed data. The positions

(16) Poojary, D. M.; Bortun, A. I.; Bortun, L. N.; Clearfield, A. *Inorg. Chem.* **1997**, *36*, 3072.

(17) Dadachov, M. S.; LeBail, A. *Eur. J. Solid State Inorg. Chem.* **1997**, *34*, 381.

(18) Williams, W. J. *Handbook of Anion Determination*; Butterworth: London, 1984.

(19) Visser, J. W. *Appl. Crystallogr.* **1969**, *2*, 89.

(20) Larson, A.; Dreele, R. B. *GSAS: Generalized Structure Analysis System*; LANSCE, Los Alamos National Laboratory, Los Alamos, NM; Copyright 1985−88 by the Regents of the University of California.

(21) Le Bail, A.; Duroy, H.; Fourquet, J. L. *Mater. Res. Bull.* **1988**, *23*, 4467.

Table 1. Crystallographic Data for Titanium Trisilicate Phases

formula	$K_2TiSi_3O_9 \cdot H_2O$	$K_{1.26}H_{0.74}TiSi_3O_9 \cdot 1.8H_2O$
fw	372.36	356.28
space group	$P2_12_12_1$ (no. 19)	$P2_1/c$ (no. 14)
a (Å)	9.9081(4)	7.2219(1)
b (Å)	12.9445(5)	10.0354(2)
c (Å)	7.1384(3)	12.9278(2)
β (deg)		91.447(1)
V (A^3)	915.5	936.63
Z	4	4
d_{calc} (g/cm^3)	2.701	2.523
pattern range (2θ) (deg)	10−90	9.5−85
no. of reflections	458	662
expected R_{wp}	0.033	0.032
R_{wp}	0.148	0.140
R_p	0.109	0.101
R_F	0.042	0.037

Table 2. Positional and Thermal Parameters for $K_2[TiSi_3O_9] \cdot H_2O$

atom	x	y	z	U_{iso},[a] Å^2
Ti1	0.4548(4)	0.2123(2)	0.2573(4)	0.029(1)
Si1	0.1809(6)	0.1735(4)	0.0048(6)	0.034(2)
Si2	0.0378(6)	0.0462(3)	0.7302(7)	0.036(2)
Si3	0.6419(6)	0.3316(4)	0.5814(6)	0.036(2)
O1	0.4171(7)	0.3672(4)	0.2439(10)	0.014(3)
O2	0.3359(7)	0.1869(6)	0.0410(9)	0.046(4)
O3	0.5145(8)	0.0664(4)	0.2693(11)	0.033(4)
O4	0.5666(9)	0.2406(5)	0.4858(9)	0.023(4)
O5	0.6152(7)	0.2290(6)	0.0946(9)	0.015(3)
O6	0.2966(7)	0.1886(6)	0.4289(9)	0.024(4)
O7	0.0992(8)	0.1539(5)	0.1982(7)	0.021(3)
O8	0.0956(9)	0.0582(5)	0.5237(9)	0.013(3)
O9	0.1593(8)	0.0724(5)	0.8776(10)	0.024(3)
K1	0.2069(5)	0.6335(3)	0.1527(5)	0.055(2)
K2	0.4294(5)	0.0798(2)	0.7045(5)	0.045(2)
O10[b]	0.6858(12)	0.662(6)	0.8840(12)	0.046(4)

[a] $U_{iso} = B_{iso}/8\Pi^2$. [b] Water oxygen atom

of the potassium atom and that of the water oxygens were derived from Fourier difference maps. The maps also showed a peak close to the center of symmetry which however did not refine well. It is possible that it may represent the position of a partial oxygen atom occupancy of a disordered water molecule resulting from the nonstoichiometric amount of water present, 1.88 mol from TGA and 1.8 from X-ray refinement. The structure was then refined as described above for compound I. Crystallographic and experimental parameters are given in Table 1 and the positional and thermal parameters in Tables 2 and 3.

The space group $P2_1/c$ is not a subgroup of $P2_12_12_1$ a point that is somewhat unusual for two such closely related structures. Therefore, we carried out a solution for compound II ab initio from the powder data. The structure factor amplitudes were extracted from the profile by the Le Bail method[21] using the program EXTRA.[22] The profile R factor for the extraction was 0.127. The intensities of 208 independent reflections (31% of the total possible observations) were input to SIRPOW.92,[23] a direct methods program for the solution of unknown crystal structures using powder data. An E-map calculated for a set with the best figure of merit (CFOM = 0.95) yielded the positions of all the atoms except two oxygen atoms, one corresponding to the silicate groups and the other to the lattice water. The atomic positions obtained from the E-map are strikingly similar to those obtained above for the same

(22) Altamare, A.; Burla, M. C.; Cascarano, G.; Giacovazzo, C.; Guagliardi, A.; Moliterni, A. G. G.; Polidori, G. *J. Appl. Crystallogr.* **1995**, *28*, 842.

(23) Altamare, A.; Cascarano, G.; Giacovazzo, C.; Guagliardi, A.; Burla, M. C.; Polidori, G.; Camalli, M. SIRPOW.92; Istituto di Ricerca per lo Sviluppo di Metodologie, Cristallografiche CNR: Bari, Italy, 1992.

Table 3. Positional and Thermal Parameters for $K_{1.26}H_{0.74}[TiSi_3O_9] \cdot 1.8H_2O$

atom	x	y	z	U_{iso}, Å^2
Ti1	0.2617(5)	0.7062(4)	0.2056(2)	0.029(3)
Si1	0.0127(7)	0.4344(6)	0.1743(4)	0.015(5)
Si2	0.7253(7)	0.2962(7)	0.0469(3)	0.014(5)
Si3	0.4211(7)	0.4040(6)	0.1714(4)	0.019(5)
O1	0.2449(12)	0.6816(9)	0.3640(6)	0.004(4)
O2	0.0417(11)	0.5915(8)	0.1897(7)	0.015(4)
O3	0.2571(11)	0.7562(8)	0.0668(5)	0.009(4)
O4	0.4777(12)	0.8224(10)	0.2338(6)	0.001(4)
O5	0.0879(11)	0.8649(9)	0.2259(6)	0.009(4)
O6	0.4281(11)	0.5618(7)	0.1950(6)	0.012(4)
O7	0.2049(9)	0.3600(9)	0.1567(7)	0.010(4)
O8	0.5219(9)	0.3659(8)	0.0632(5)	0.005(4)
O9	0.8804(10)	0.4114(8)	0.0734(7)	0.008(4)
K2	0.7445(7)	0.7045(6)	0.0955(3)	0.089(5)
O10[a]	0.0656(26)	0.4554(21)	0.4241(8)	0.217(10)
O11[b]	0.2718(20)	0.4574(18)	0.606(10)	0.167(7)

[a] Water oxygen atom. [b] This site is partially filled with K^+ ions and water oxygen with occupancies of about 0.2 and 0.8, respectively.

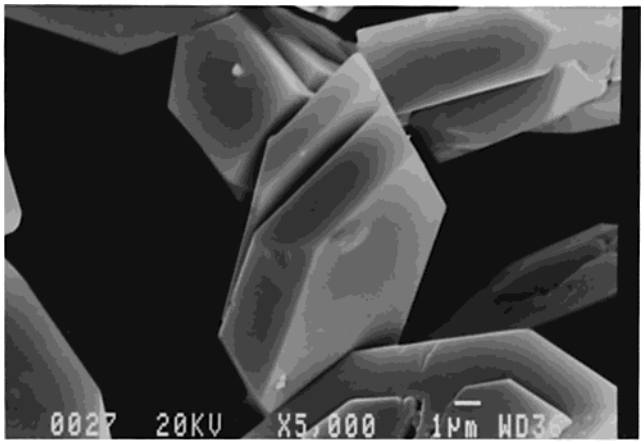

Figure 1. Electron micrograph at 5000× magnification showing the morphology of the hydrothermally grown crystals of $K_2TiSi_3O_9 \cdot H_2O$.

structure. The relationship of the ab initio derived parameters to those in Table 3 are $^1/_2 + x, y, z$. For example, the Ti parameters obtained by direct methods (unrefined) are −0.245, 0.293, and 0.206 which transform into 0.255, 0.707, and 0.206. These values match those in Table 3 closely. The R factor for these atoms was 20%. These positions were then transferred to GSAS for full pattern refinement. The positions of two missing oxygen atoms were located from difference Fourier maps following initial refinement of the profile functions, cell parameters, background functions, and zero point errors. These results lend confidence that removal of almost half the K^+ leads to a symmetry change.

Results

Synthesis. The electron micrograph at 5000× magnification, presented in Figure 1, shows the morphology of the hydrothermally grown crystals of $K_2TiSi_3O_9 \cdot H_2O$. Elemental analysis of compound I gave 21.2% K, 12.7% Ti, and 22.5% Si. Calculated for $K_2TiSi_3O_9 \cdot H_2O$: 20.97% K, 12.90% Ti, 22.58% Si. The potassium phase was exchanged with protons by treatment with a 0.5 M CH_3-COOH solution. It was found that mineral acid treatment results in a gradual decrease of the exchanger crystallinity. Two titanium silicates partially converted into the protonic form were prepared. For the first partially exchanged sample, found: Ti, 13.3%; Si, 23.2%; K, 13.5%. Calculated for $K_{1.26}H_{0.74}TiSi_3O_9 \cdot 1.8\ H_2O$: Ti,

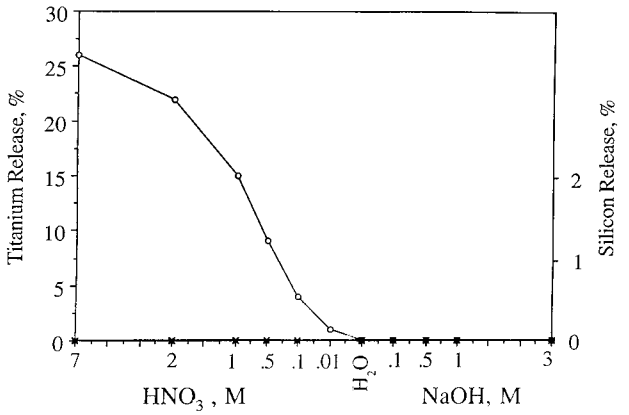

Figure 2. Dissolution of titanium (○) in acid solution, and silicon (■) in basic solution from $K_2TiSi_3O_9 \cdot H_2O$.

13.36%; Si, 23.49%; K, 13.74%. For the second exchanger, compound III, elemental analysis gave: Ti, 14.7%; Si, 25.8%; K, 3.6%. Calculated for $K_{0.3}H_{1.7}TiSi_3O_9 \cdot 2.4H_2O$: Ti, 14.39%; Si, 25.31%; K, 3.52%.

Before carrying out the exchange of protons for K^+ to produce the protonated phases, we examined the stability of compound I in acid and base solutions. The results are given in Figure 2. $K_2TiSi_3O_9 \cdot H_2O$ was found to be hydrolytically stable in alkaline media. No titanium was detected in alkaline solutions and only a trace amount of silicate release was found. No silicate release from $K_2TiSi_3O_9 \cdot H_2O$ was found also in acid media. However, $K_2TiSi_3O_9 \cdot H_2O$ undergoes a substantial chemical decomposition when it is contacted with HNO_3, which results in titanium release into solution and a gradual conversion of the crystals to an amorphous product. Compound I loses 3% titanium in 0.1 M HNO_3, about 15% titanium in 1 M HNO_3 and about 25% titanium in 7 M HNO_3. This indicates that $K_2TiSi_3O_9 \cdot H_2O$ cannot be used in acid media with acid concentrations higher than 0.01−0.05 M. However, using acetic acid to exchange protons into the lattice kept the pH high enough to avoid dissolution of Ti. Since the acid concentration was 0.5 M, the extent of exchange of H^+ for K^+ depended upon the contact time at a constant pH of ∼2.5.

Figure 3 contains the thermogravimetric weight loss curves for the framework titanium silicate phases I and III. The total weight loss for the potassium phase $K_2TiSi_3O_9 \cdot H_2O$ was 4.94% and the final product should have the formula $K_2TiSi_3O_9$ (fw = 354.4). Thus, the formula weight initially was 372.8. On the assumption that this increase in weight is due totally to water, the original solid contained 1.0 mol of H_2O as indicated. The weight loss occurs in one step. It starts at 160 °C and ends at 365 °C. We attribute this weight loss to zeolite-type water. According to the X-ray diffraction data, $K_2TiSi_3O_9 \cdot H_2O$ undergoes a phase transition above 600 °C with the formation of a crystalline phase $K_2TiSi_3O_9$, referred to as wadeite, in which the linear chains have cyclized to form rings.[24] In the new phase the formerly exchangeable cations are no longer mobile and permanently fixed in the structure.

The protonic phase III (Figure 3b) yielded a total weight loss of 17.71% which corresponds to the weight loss expected for the formula $K_{0.3}H_{1.7}TiSi_3O_9 \cdot 2.4H_2O$.

(24) Bragg, L. *The Crystalline State*; Cornell University Press: Ithaca, NY, 1965.

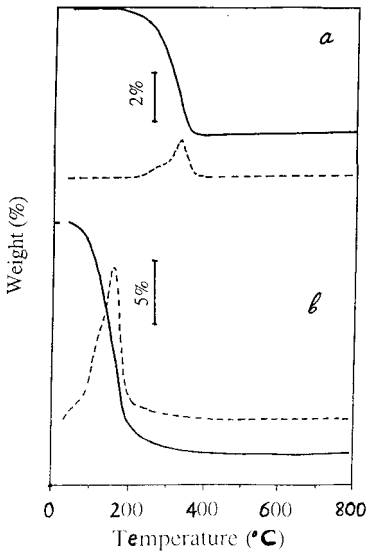

Figure 3. TG curves of $K_2TiSi_3O_9 \cdot H_2O$ (a) and $K_{0.3}H_{1.7}TiSi_3O_9 \cdot 2H_2O$ (b).

The weight loss occurs in two steps in the temperature range 40−390 °C. First, 2.4 mol of crystal water (13.3%) and then 0.85 mol of structurally bound water (4.58%), due to the condensation of hydroxyl functional groups, are released. Under the conditions of the experiment it was not possible to separate the steps although the differential curve exhibits a broad shoulder on the low-temperature side. The TGA curve for phase II also showed a one step weight loss of 9.2% corresponding to 1.88 mol of water.

Structures of $K_2TiSi_3O_9 \cdot H_2O$ and the Partially Protonated Phases. Positional and thermal parameters of I and the partially protonated phase II are presented in Tables 2 and 3, respectively, whereas the bond lengths and angles are given in Table 4. Table 5 lists the potassium−oxygen interatomic distances in both the titanium and zirconium analogues. The final Rietveld refinement differences plots are shown in Figures 4 and 5.

The trisilicate group, $Si_3O_9^{6-}$, forms linear chains that run parallel to the *c* axis in I and the *a* axis in II. In the chain, Si1 is connected to Si2 by O9 and Si2 is linked to Si3 by O8 (Figure 6). Oxygen, O7 then links Si3 to Si1 and hence the polymeric chain extends infinitely in the *c* direction. The Ti atoms are octahedrally coordinated by the remaining oxygen atoms of the trisilicate group and serve to link the silicate chains together into the three-dimensional framework. In the *ab* plane (Figure 7a) silicate groups share oxygens with Ti atoms forming alternating octahedra and tetrahedra sharing corners. This is best seen in Figure 8 in polyhedral representation. This arrangement of polyhedra together with the $(Si_3O_9)^{6-}$ polymeric chains form two types of tunnels running parallel to the *c* axis in the orthorhomic structure (parallel to the *a* direction in the monoclinic). The larger tunnel has a 16-atom opening, 4 Ti, 4 Si, and 8 O. Each large tunnel is surrounded by four smaller tunnels with 12-atom openings and they are in turn surrounded by four larger tunnels. The tunnels are connected to each other through 14-atom openings illustrated in Figure 6. These openings lie approximately parallel to the *ab* diagonal perpendicular to the *ab* plane.

Table 4. Bond Lengths (Å) and Angles (deg) for the Titanium Compounds I and II

bond	phase I	phase II	bond	phase I	phase II
Ti1−O1	2.042(6)	2.069(8)	Ti1−O2	1.970(6)	1.968(8)
Ti1−O3	1.981(6)	1.862(7)	Ti1−O4	2.005(6)	1.974(8)
Ti1−O5	1.980(6)	2.049(8)	Ti1−O6	2.013(6)	1.890(8)
Si1−O2	1.566(7)	1.602(8)	Si1−O5	1.589(7)	1.651(7)
Si1−O7	1.620(7)	1.598(7)	Si1−O9	1.607(6)	1.614(7)
Si2−O1	1.650(7)	1.638(8)	Si2−O3	1.572(6)	1.569(7)
Si2−O8	1.589(7)	1.646(7)	Si2−O9	1.634(7)	1.640(8)
Si3−O4	1.553(7)	1.631(7)	Si3−O6	1.557(8)	1.613(8)
Si3−O7	1.640(6)	1.629(7)	Si3−O8	1.676(7)	1.638(7)
O1−Ti1−O2	91.0(3)	88.0(4)	O1−Ti1−O3	173.2(4)	170.2(4)
O1−Ti1−O4	87.7(3)	87.3(4)	O1−Ti1−O5	90.7(3)	85.1(3)
O1−Ti1−O6	92.0(3)	91.9(4)	O2−Ti1−O3	93.1(3)	93.6(4)
O2−Ti1−O4	176.7(4)	175.2(4)	O2−Ti1−O5	92.2(3)	88.4(4)
O2−Ti1−O6	89.2(3)	93.3(4)	O3−Ti1−O4	88.5(3)	90.8(4)
O3−Ti1−O5	83.7(3)	85.3(4)	O3−Ti1−O6	93.5(3)	97.6(4)
O4−Ti1−O5	90.8(4)	90.1(5)	O4−Ti1−O6	87.9(3)	88.0(4)
O5−Ti1−O6	176.9(4)	176.5(4)			
O2−Si1−O5	112.8(5)	112.2(6)	O2−Si1−O7	111.5(5)	111.5(6)
O2−Si1−O9	108.3(5)	108.3(5)	O5−Si1−O7	107.5(5)	108.3(5)
O5−Si1−O9	109.9(5)	108.0(6)	O7−Si1−O9	106.7(5)	108.5(5)
O1−Si2−O3	111.8(5)	114.3(6)	O1−Si2−O8	107.4(5)	108.0(5)
O1−Si2−O9	108.7(4)	105.7(5)	O3−Si2−O8	112.0(5)	110.9(5)
O3−Si2−O9	108.7(5)	111.2(5)	O8−Si2−O9	108.2(5)	106.3(6)
O4−Si3−O6	108.9(6)	109.8(5)	O4−Si3−O7	112.6(5)	111.2(6)
O4−Si3−O8	108.5(5)	108.9(5)	O6−Si3−O7	108.6(5)	108.3(5)
O6−Si3−O8	113.1(5)	112.2(6)	O7−Si3−O8	105.1(5)	106.4(5)
Si1−O9−Si2	129.1(6)	131.1(6)	Si2−O8−Si3	126.6(5)	128.8(5
Si3−O7−Si1	132.1(6)	133.7(6)			

Table 5. A Comparison of K^+ Ion Environments in Zr and Ti Trisilicate Compounds

bond	$K_2ZrSi_3O_9 \cdot H_2O$	$K_2TiSi_3O_9 \cdot H_2O$	difference
K1−O1	3.21(1)	3.17(1)	0.04
K1−O3	3.14(1)	2.95(1)	0.19
K1−O4	2.93(1)	2.82(1)	0.10
K1−O5	2.96(1)	2.81(1)	0.15
K1−O6	2.87(1)	2.80(1)	0.07
K1−O7	3.39(1)	3.22(1)	0.17
K1−O10	2.58(1)	2.61(1)	−0.03
K2−O2	2.90(1)	2.92(1)	−0.02
K2−O3	3.33(1)	3.22(1)	0.11
K2−O4	2.99(1)	2.94(1)	0.05
K2−O6	2.84(1)	2.75(1)	0.09
K2−O7	3.09(1)	3.04(1)	0.05
K2−O8	2.95(1)	2.91(1)	0.04
K2−O9	3.08(1)	2.95(1)	0.13
K2−O9B	3.30(1)	3.18(1)	0.12
K2−O10	2.91(1)	2.85(1)	0.06

The K^+ ion, K1, and water oxygen, O10, are located in the large pore. Potassium ion, K1, is surrounded by five oxygens (O3A, O4A, O5A, O6, and O10C) and the corresponding K−O bond distances are in the range 2.6−3.2 Å (Figure 9). This potassium also has four relatively longer contacts, one with the symmetry related O4 atom (3.38 Å), O1(3.17 Å), O7D (3.22 Å), and O8E (3.39 Å). The K^+ ion, K2, occupies the cavities within the small channels. K2 is close to six oxygen atoms where the K−O distances are in the range 2.75−2.95 Å (Table 5) and three, O7E, O9B, O3, are at distances greater than 3 Å (Figure 9).

The structure of compound II is similar to that of compound I in terms of the metal silicate network. This is illustrated in Figure 7a where the view is looking down the tunnels (*ab* plane for compound I and *bc* plane for compound II). The two types of tunnels are clearly shown in both representations but the monoclinic structure is shifted $^1/_4$ along the horizontal axis (b_m or a_o). Mild acid treatment of compound I exchanged about 80% of the potassium ions in the larger tunnel, corresponding to the K1 site, for protons. In compound II, this exchange site is denoted by O11 (Table 3). By analogy with compound I, this site should then have 0.26 occupancy for K^+ ions and 0.74 for water oxygens. It is highly probable that the charge balancing protons (0.8) are present combined with the water molecule as $O11H_3O^+$ (see NMR and IR sections). Both this ion/water site and the water oxygen position (O10) are shifted by about 1 Å relative to their positions in compound I. The remaining potassium ions, K2, are in the small tunnels.

The X-ray diffraction powder pattern of $K_{0.3}H_{1.7}TiSi_3O_9 \cdot 2.4H_2O$ (III) is shown in Figure 10A. We note that many new reflections are present and the intensities are much lower than those of the parent phase, compound I, and the peak shapes are distorted. This latter feature kept us from being able to properly decompose the pattern for a Rietveld-type structure solution and refinement. In addition the pattern does not correspond to a mixture containing either phase I or II. However, by exchange with KCl + KOH to the point where the composition is close to $K_2TiSi_3O_9 \cdot H_2O$ (pH ≅ 10) the X-ray pattern (Figure 10A) reverts to that of the starting phase I (Figure 10B). The peak shapes are once again regular, the background has decreased, and the intensities increased substantially over those of the highly protonated phase. Thus, the framework remains in tact as the K^+ is replaced by protons whether the X-ray pattern is that of a single phase or a mixture of phases.

NMR Spectra. ^{29}Si MAS NMR spectra with ^1H decoupling are shown in Figure 10. According to these spectra, $K_2TiSi_3O_9 \cdot H_2O$, which originally appeared to have a single resonance, on scale expansion actually exhibits three resonances at −85.1, −85.4, and −86.6 ppm (spectrum a in Figure 11). $K_{1.26}H_{0.74}TiSi_3O_9 \cdot 1.6H_2O$ contains two types of silicon atoms with almost similar environments, but the expanded scale spectrum (Figure 11b) indicates a shoulder on the high-field side indicative of a third resonance. The position of the ^{29}Si NMR

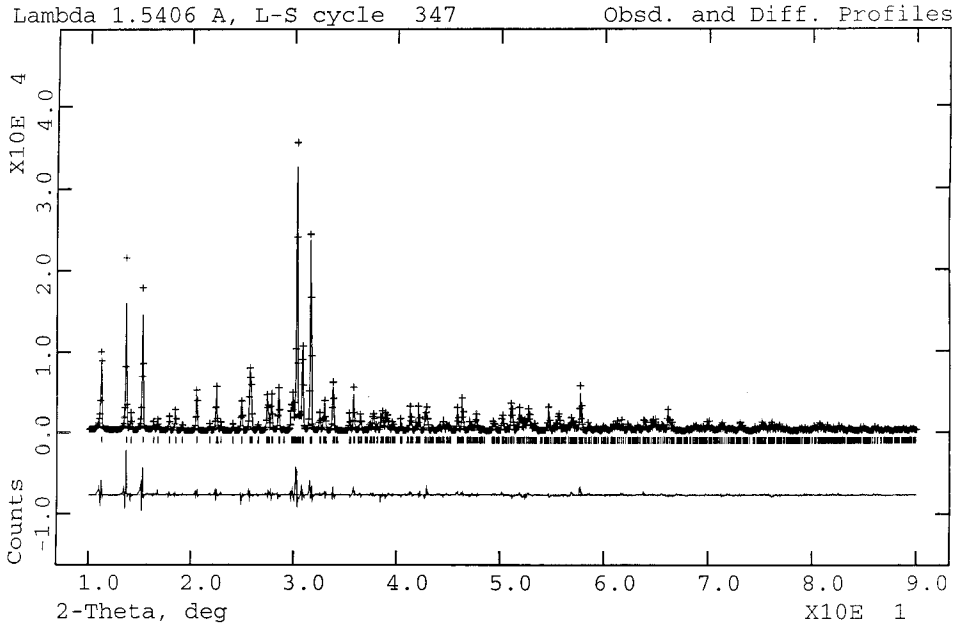

Figure 4. Observed (+) and calculated (−) profiles for the Rietveld refinement for compound I. The bottom curve is the difference plot on the same intensity scale and the tick marks indicate the positions of calculated reflections.

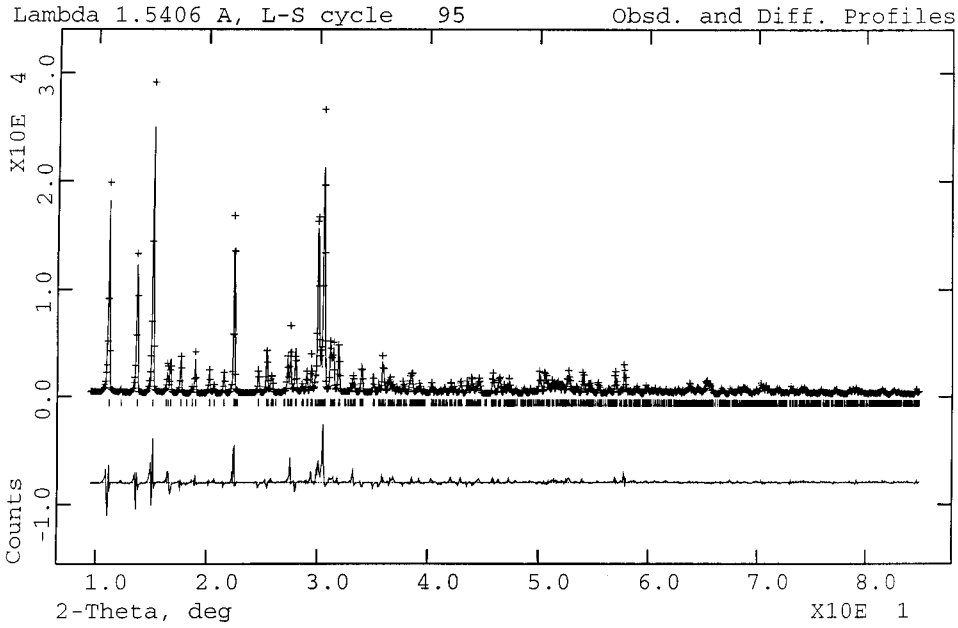

Figure 5. Rietveld difference plot for compound II.

peaks for $K_2TiSi_3O_9 \cdot H_2O$ are shifted in $K_{1.26}H_{0.74}TiSi_3O_9 \cdot 1.8H_2O$ to stronger field with two peaks at −87.1 ppm and −89.3 and a shoulder at −90.5 ppm. By analogy with zeolites[25] and ETS-10,[26,27] these peaks could be assigned to silicon coordinated with two silicon and two titanium atoms (2 Si, 2 Ti) with the Si in slightly different environments. In fact reference to Figure 6 shows that this is the case. The upfield shift of about 4 ppm (from −85.4 to −90.0 ppm) of the ^{29}Si NMR signal, as the $K_2TiSi_3O_9 \cdot H_2O$ sample is converted to about 35−40% into the proton form, indicates that the hydroxyl functional groups in the exchanger belong rather to silicon than to titanium atoms.[15]

The ^{29}Si MAS NMR spectrum of $K_{0.3}H_{1.7}TiSi_3O_9 \cdot 2.4H_2O$ (Figure 11c) is much more complex. It has eight NMR signals at −86.2, −89.6, −92.4, −94.7, −97.3, −98.7, −100.1, and −108.5 ppm. Such a diversity could be a result of the disordering of the titanium silicate lattice, creating different coordination states for the silicon and the positioning of the protons on the lattice creating a hydrogen bonding network. In addition two of the peaks appear to be doublets. The effect of this H^+ positioning was probed by cross-polarization NMR (Figure 11d−f). Almost no change was observed in the spectrum for II but two of the peaks at −89.6 and −92.4 ppm were eliminated from the spectrum for compound III and the peaks are not split. Additional work is in progress to clarify this behavior.

(25) Lippmaa, E.; Mägi, M.; Samoson, A.; Engelhard, G.; Grimmer, A.-R. *J. Am. Chem. Soc.* **1980**, *102*, 4889.
(26) Anderson, M. W.; Terasaki, O.; Ohsuna, T.; Phillippou, A.; Mackay, S. P.; Ferreira, A.; Rochca, J.; Lidin, S. *Nature* **1994**, *367*, 347.
(27) Das, T. K.; Chandwadkar, A. J.; Budhkar, A. P.; Sivasanker, S. *Microporous Mater.* **1996**, *5*, 401.

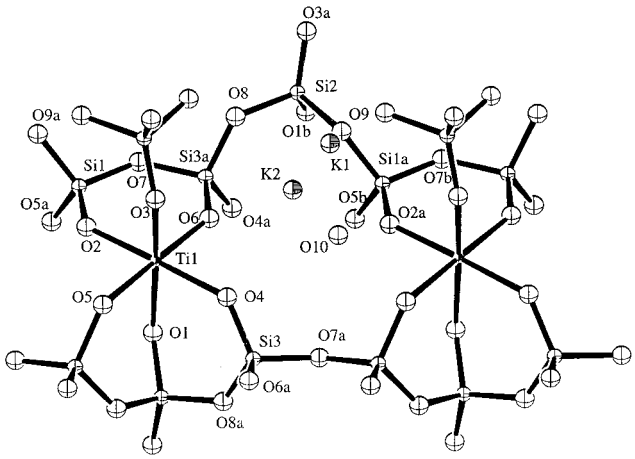

Figure 6. A portion of the structure of compound I showing atom labeling and metal coordination. The view is approximately along the [110] direction and the *c* axis is horizontal. This view clearly shows the 14-membered rings connecting the small and large channels. If the *c* axis is turned in the vertical direction the atoms are approximately centered along the *ab* diagonal in the orthorhombic cell.

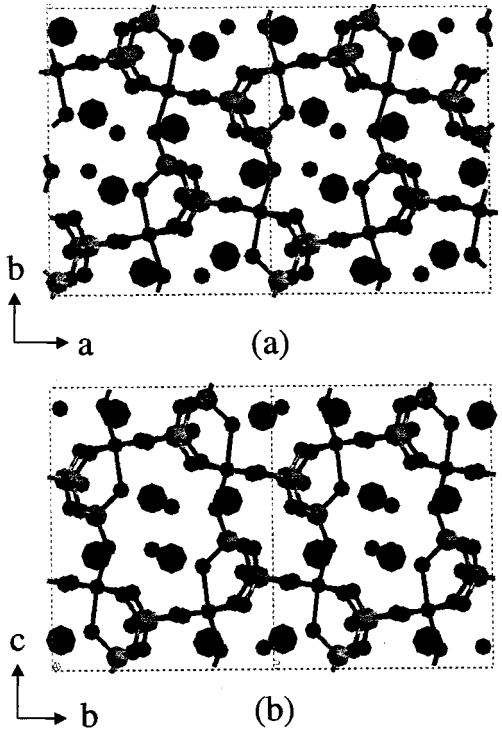

Figure 7. Ball and stick representation of compound I, orthorhombic (a) and compound II, monoclinic (b) as viewed down the *c* axis. A shift of I by $^1/_4$ along the *a* axis very nearly reproduces structure b. The larger atoms within the tunnels are K^+ and the smaller atoms reprsent water molecules.

IR Spectra. The infrared spectra of the framework potassium titanium silicate, $K_2TiSi_3O_9 \cdot H_2O$, and its proton form, $K_{0.3}H_{1.7}TiSi_3O_9 \cdot 2.4H_2O$, both air-dried, are presented in Figure 12 and their band positions are listed in Table 6. The spectrum $K_{0.3}H_{1.7}TiSi_3O_9 \cdot 2.4H_2O$ (curve b) contains a complex hydroxyl stretching band and the bending vibration. At least five components of the band are recognizable and indicate the presence of free water (3570, 3530, 3384, and 1640 cm[1]) and H_3O^+ (3250−3100 cm^{-1}). In addition, the presence of SiO−H hydroxyl stretching bands may also be present. The potassium phase spectrum (a) distinctly shows the

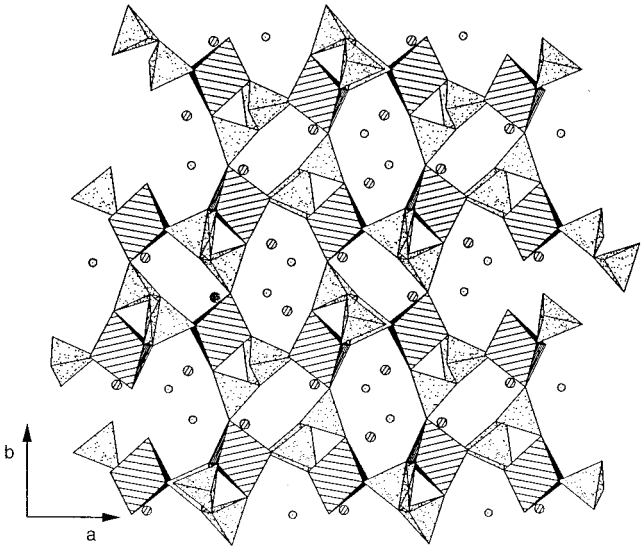

Figure 8. A polyhedral representation of the structure of compound I as viewed down the *c* axis showing the ions and water molecules in the channel. Solid lines in octahedra depict Ti polyhedra and stippled groups represent silicon tetrahedra. K1 and K2 ions are shown by lined circles and water molecules by open circles in the large and small cavities.

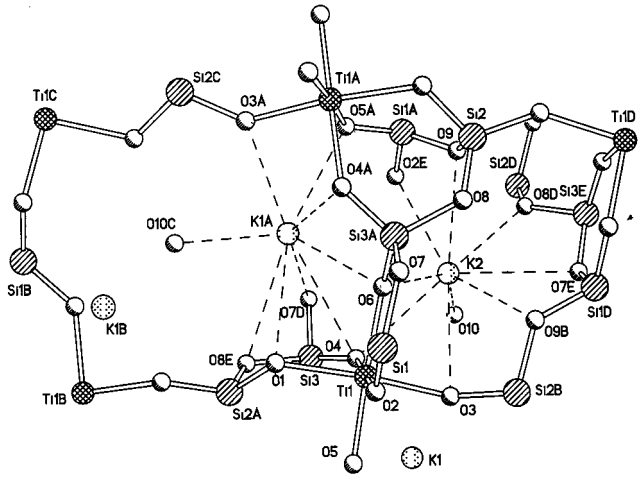

Figure 9. A ball-and-stick representation of the potassium ion coordination in compound I. K1 is in the larger tunnel and K2 in smaller one. The very long interatomic distances (greater than 3.0 Å) are O1, O7D, O4, O8E to K1 and O7E, O9B, and O3 to K2.

presence of the crystal water (3270, 3110, and 1635 cm^{-1}). The bands at 1103, 1026, 952, and 893 cm^{-1} for $K_2TiSi_3O_9 \cdot H_2O$, and at 1124, 1077, 1001, and 920 cm^{-1} for $K_{0.3}H_{1.7}TiSi_3O_9 \cdot 2.4H_2O$, are most likely the SiO_4 asymmetric and symmetric vibrations.[28,29] The difference in the position of the bands observed for titanium silicate in potassium and protonic forms supports the point that the hydroxyl functional groups are coordinated with silicon atoms.

Ion Exchange Behavior. The replacement of potassium ion by protons in $K_2TiSi_3O_9 \cdot H_2O$ is essentially an ion exchange reaction. According to the chemical formula of the proton phase, $K_{0.3}H_{1.7}TiSi_3O_9 \cdot 2.4H_2O$, the

(28) Lasarev, A. N. *Vibrational Spectra and Structure of Silicates* (English Translation); Consultants Bureau: New York, 1972.
(29) Boccuti, M. R.; Rao, K. M.; Zecchina, A.; Leofanti, G.; Petrini, G. *Stud. Surf. Sci. Catal.* **1990**, *48*, 133.

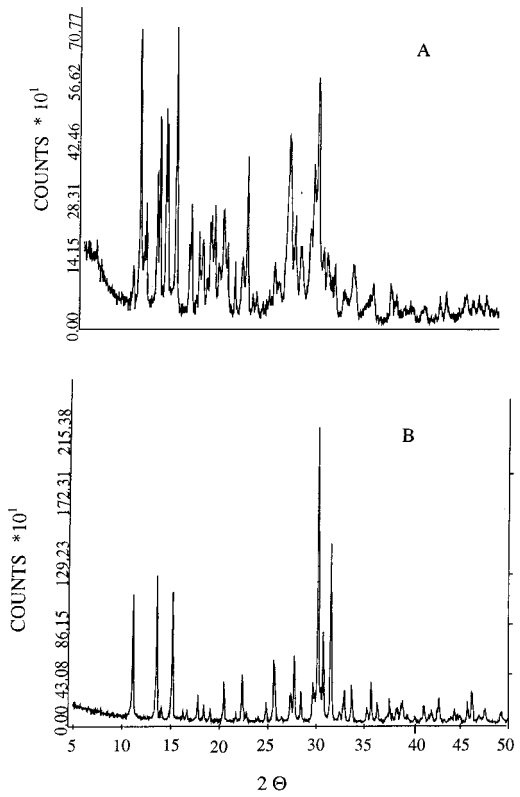

Figure 10. X-ray powder pattern of $K_{0.3}H_{1.7}TiSi_3O_9 \cdot 2H_2O$ (A) and the same compound treated with KCl + KOH to exchange K^+ for H^+ (B). Pattern B resembles that for $K_2TiSi_3O_9 \cdot H_2O$ (Figure 4). Note the much higher intensities in pattern B.

calculated ion exchange capacity is 5.11 mequiv/g, assuming that only the protons exchange. The results of potentiometric titrations carried out with MCl-MOH solutions (M = alkali metal) by static equilibrations are shown in Figure 13a. Each ion exhibits a different shaped curve. About 0.75 mequiv/g of Cs^+ is taken up at a pH of 3.0 and the equilibrium uptake increases as a function of pH to reach a maximum of 2.0 mequiv/g at pH 12. Lithium and sodium ion exchange are similar but differ from that for cesium. Li^+ and Na^+ uptake starts at a pH about 3.0−3.5 and their exchange increases gradually with pH increase, reaching a maximum value of 4.3−4.5 mequiv/g at pH 9.5−10.0. Potassium is the most preferred ion over the pH range 3−12. Its uptake starts at a pH of higher than 2 and increases to 1.3 mequiv/g with increase of the pH to 4. The uptake increases slowly with further increase of pH to 6, whereupon a large increase in uptake occurs at a relatively small pH change. Further exchange takes place in alkaline solution reaching the theoretically possible value of the ion exchange capacity (IEC), 5.3 mequiv/g at pH 9.

Titration curves for alkaline earth cations are shown in Figure 13b. These data show extremely low divalent metals uptake in comparison with alkali metals. Alkaline earth metal cation exchange starts at a pH between 4 and 5. Their uptake is only 0.4−0.7 mequiv/g in the pH range 7−9 independent of the cation used. Maximum IEC values of 1.5−1.8 mequiv/g were found at pH 12.0, where the precipitation of alkali metals in the form of insoluble carbonates and hydroxides is to be expected.

Taking into consideration the framework structure of $K_2TiSi_3O_9 \cdot H_2O$ and its proton form and the size of the

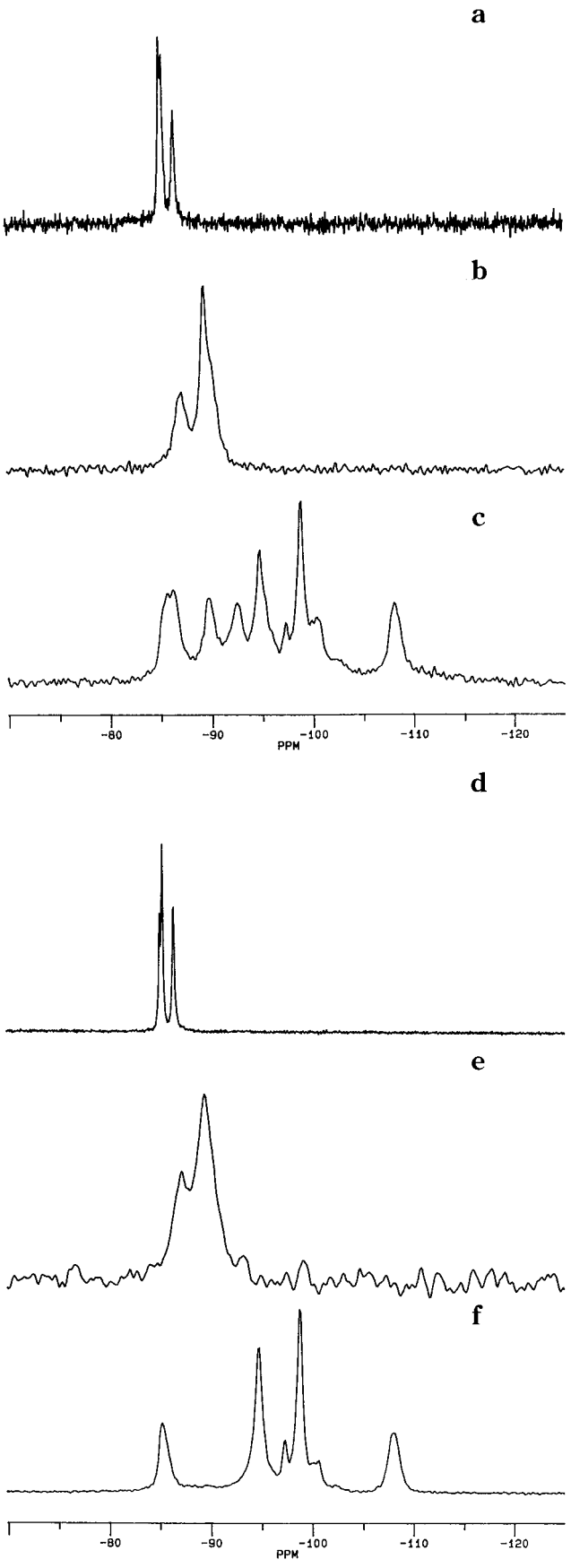

Figure 11. The ^{29}Si MAS NMR spectra, ^1H decoupled, of $K_2TiSi_3O_9 \cdot H_2O$ (a), $K_{1.26}H_{0.74}TiSi_3O_9 \cdot 2.4H_2O$ (b), $K_{0.3}H_{1.7}TiSi_3O_9 \cdot 2H_2O$ (c), and cross-polarized spectra of these compounds in d, e, and f.

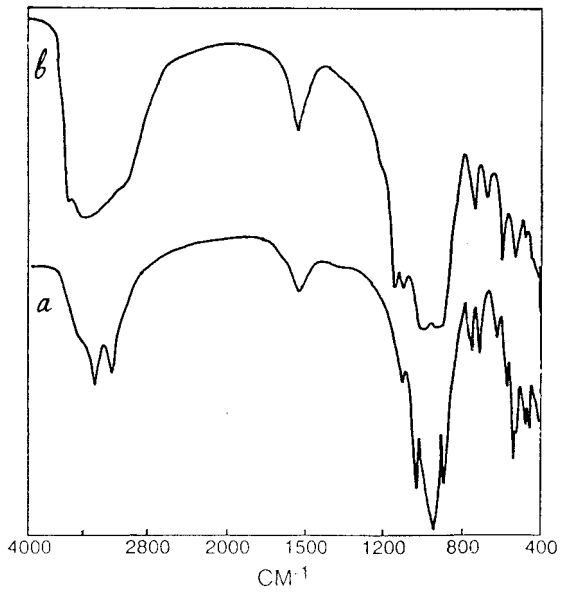

Figure 12. The IR spectra of $K_2TiSi_3O_9 \cdot H_2O$ (a) and $K_{0.3}H_{1.7}TiSi_3O_9 \cdot 2.4H_2O$ (b).

Table 6. Positions of Peaks (cm^{-1}) in IR Spectra of the Framework Titanium Silicates

$K_2TiSi_3O_9 \cdot H_2O$	$K_{0.3}H_{1.7}TiSi_3O_9 \cdot 2H_2O$
3270	3570
3110	3531
1635	3384
1103	3250
1026	3100
952	1640
893	1124
752	1077
711	1001
626	920
575	678
547	596
487	530
461	411

openings to the channels, the experimental data for divalent cations can be explained by a blocking of channel entrances leading to the inner parts of exchanger assuming exchange occurs with the fully hydrated cations and that phase III retains the same channel system as phases I and II. As evidence for this point, we cite the data on some transition metal ions uptake by phase III. Some ion exchange isotherms are presented in Figure 13. The exchange of Co^{2+} (pH 5.4−5.8) is relatively low (0.5 mequiv/g from 0.1 M solution)

Table 7. Cesium and Strontium Uptake by Framework Titanium Trisilicates from Groundwater Simulant

sorbent	K_dCs (mL/g)	K_dSr (mL/g)
$K_2TiSi_3O_9 \cdot H_2O$	280	10
$K_{1.26}H_{0.74}TiSi_3O_9 \cdot 2H_2O$	14 900	100
$K_{0.3}H_{1.7}TiSi_3O_9 \cdot 2H_2O$	>200 000	280

and does not exceed the IEC values for alkaline earth metals (Figure 13b). No Cr^{3+}(pH 3.8−2.6) or Ni^{2+}(pH 6.0−6.3) uptake was obtained. These unhydrated transition metal ions have small ionic radii and should exchange if unhydrated. However, it is likely that the exchange reaction does not generate sufficient energy to overcome the hydration energy of the cations. The only exception is copper uptake (IEC 2.7 mequiv/g). This uptake could result from a partial precipitation of copper in the form of $Cu(OH)_2$ (pH 4.3−5.6).

The extremely high affinity of $K_{0.3}H_{1.7}TiSi_3O_9 \cdot 2.4H_2O$ for monovalent cations and the lack of affinity for hydrated di- and trivalent metals could be used for analytical purposes, particularly for the separation of these elements. As an example we obtained data on the purification of 1 M $SrCl_2$ solution from potassium (17 ppm). The amount of K^+ ion in solution was two times greater than the permissible level for $SrCl_2$ of analytical grade. A total of 1 g of $K_{0.3}H_{1.7}TiSi_3O_9 \cdot 2.4H_2O$ decreased the amount of potassium in 100 mL of solution to 0.9 ppm, which gives a purification factor of 20 and K_d^K = 1600 mL/g.

On the basis of this preference for alkali cations we tested the titanium trisilicate (in potassium and potassium−hydrogen forms) for cesium removal from a groundwater simulant containing 100 mg/L Ca^{2+}, 10 mg/L Mg^{2+}, 15 mg/L Na^+, 5.5−6.9 mg/L Cs^+, and 4.6−4.8 mg/L Sr^{2+} (Table 7). The ion exchange capacity of $K_{0.3}H_{1.7}TiSi_3O_9 \cdot 4H_2O$ for cesium was determined in the same groundwater, but containing a higher initial concentration of cesium (26.6 ppm). A cesium adsorption isotherm is presented in Figure 15 plotted as cesium uptake versus the equilibrium concentration of cesium in solution. Analysis of the data given in Table 7 shows that the potassium titanium silicate practically does not exchange cesium, nor strontium from groundwater. Conversion of the exchanger into the protonic form results in a drastic increase of the exchanger selectivity for cesium. The greater the degree of proton substitution the greater the selectivity, reaching a maximum K_d value of >200 000 for $K_{0.3}H_{1.7}TiSi_3O_9 \cdot 2.4H_2O$. It is worth

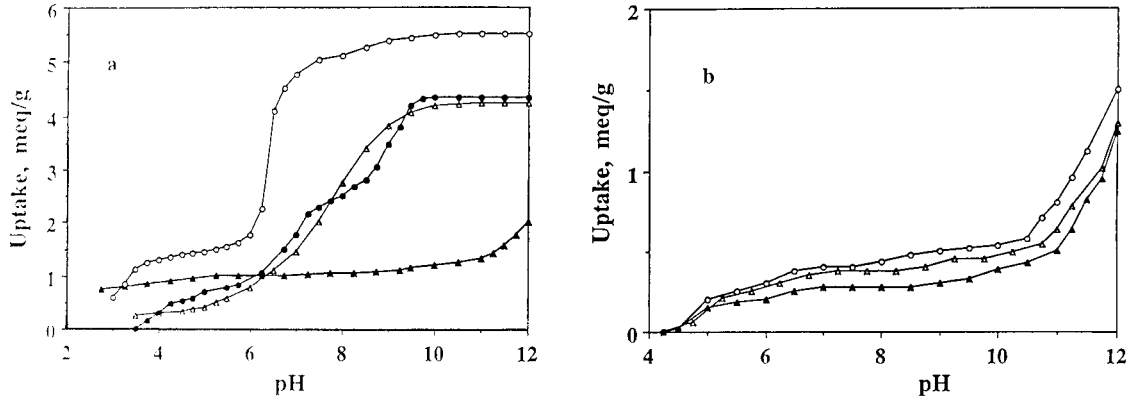

Figure 13. (a) Potentiometric titration of $K_{0.3}H_{1.7}TiSi_3O_9 \cdot 2H_2O$ with LiOH (●), NaOH (△), KOH (○), and CsOH (▲); and (b) potentiometric titration of $K_{0.3}H_{1.7}TiSi_3O_9 \cdot 2.4H_2O$ with $Ca(OH)_2$ (○), $Sr(OH)_2$ (△), and $Ba(OH)_2$ (▲).

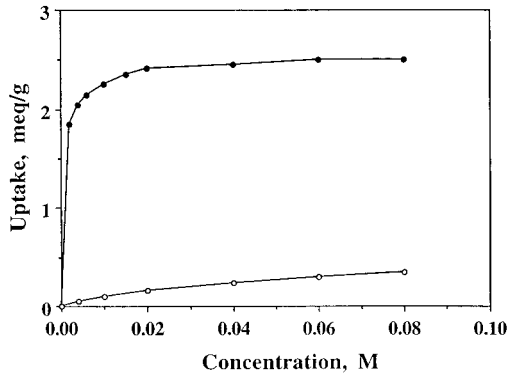

Figure 14. Transition metal ions sorption by $K_{0.3}H_{1.7}TiSi_3O_9 \cdot 2.4H_2O$: Cu^{2+} (●) and Co^{2+} (○).

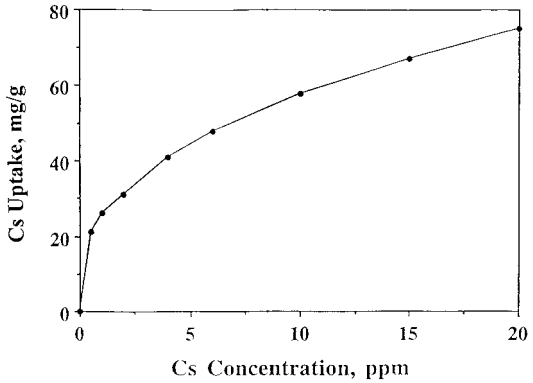

Figure 15. Cesium uptake from groundwater simulant by $K_{0.3}H_{1.7}TiSi_3O_9 \cdot 2.4H_2O$ plotted as Cs^+ remaining in solution at equilibrium as a function of cesium ion in the solid (simulant contains 26.6 ppm of Cs^+).

Table 8. K_d Values (in mL/g) of Cesium Exchange by Titanium Trisilicate Phases ($Cs^+ = 1 \times 10^{-3}$ M; $V:m$ = 200:1; t = 4 d)

sorbent	H_2O	1 M $NaNO_3$ + 0.01 M NaOH	1 M NaOH	2 M $NaNO_3$ + 1 M NaOH	5 M $NaNO_3$ + 1 M NaOH
$K_{0.3}H_{1.7}TiSi_3O_9 \cdot 2H_2O$	40 000	40	12	3	5
$K_2TiSi_3O_9 \cdot H_2O$	20	3	1	1	1

noting that the cesium capacity for this exchanger is about 70−75 mg/g (or about 25% of the uptake shown for Cs^+ in Figure 13a) which together with its high selectivity makes it suitable for use in removal of Cs^+ from groundwaters.

Because nuclear waste solutions usually contain large amounts of sodium ions, Cs^+ adsorption by the framework titanium silicate was also studied in the presence of sodium under a variety of conditions. The distribution coefficient (K_d) values characterizing the selectivity of exchangers for cesium are presented in Table 8. It is seen that $K_2TiSi_3O_9 \cdot H_2O$ does not exchange Cs^+ in any of the tested solutions. However, $K_{0.3}H_{1.7}TiSi_3O_9 \cdot 2.4H_2O$ exhibits moderately high preference for cesium in individual Cs^+ ion containing solutions, but the K_d values drop drastically in the presence of a large excess of sodium ions. This indicates that this framework titanium trisilicate does not possess a high enough affinity for cesium, as that required for treatment of highly alkaline nuclear waste.

Discussion

We had earlier determined the structure of $K_2Zr(Si_3O_9) \cdot H_2O$[16] and indicated that the corresponding titanium compound is isostructural. In the interim two X-ray studies in the titanium system were carried out. The one by Dadachov and Le Bail[17] utilized X-ray powder data in the range of 10−110° (CoKα) and yielded an orthorhombic unit cell $a = 7.1362$ (2), $b = 9.9084(3)$, $c = 12.9414$ (4) Å, space group $P2_12_12_1$. Comparison with the unit cell dimensions in Table 1 indicates agreement to within 0.03%. A single-crystal study was carried out with the mixed-cation phase $Na_{2.7}K_{5.3}Ti_4(Si_3O_9)_4 \cdot 4H_2O$. This mixed-cation phase resulted from the hydrothermal preparation because NaOH was utilized as the base and KF was added as a solubilizing agent. The phase is monoclinic, $P2_1/c$, $a = 6.3916$ (8), $b = 11.4386$ (9), $c = 12.7951$ (Å), $\beta = 104.366$ (9)°, $Z = 4$. Our monoclinic phase (Table 1) has significantly different unit cell dimensions and a smaller β angle but the volume (936.6 Å^3) is larger by 3.35% than that of the mixed Na, K phase 906.2(2) Å^3. This difference may indicate that the bulk of the protons are present as hydronium ions. This supposition arises from our study of six zirconium trisilicate phases.[16] In general the larger the ions inside the cavities the greater the unit cell volume. For example, the volume of $K_2ZrSi_3O_9 \cdot H_2O$ is 987.0 Å^3, the volumes of the phases in which 1.1 and 1.5 mol of Cs^+ have replaced a corresponding amount of K^+ are 1041.9 and 1052.8 Å, respectively. This ability to change the volume to accommodate ions of different size indicates a certain flexibility to the trisilicate framework. Framework flexibility may also allow the change in symmetry from orthorhombic to monoclinic. Compound II crystallized in space group $P2_1/c$ which is not a subgroup of $P2_12_12_1$, the space group for the potassium phase of both the Ti and Zr compounds. However, these latter two phases exhibit psuedo-symmetry as revealed by calculation with program MISSYM.[30] Most of the atoms in the $P2_12_12_1$ space group fit to an inversion center at 0.25, 0, 0.007. The only atoms that do not adhere to this symmetry are the framework oxygens 08 and 09, the water molecule 010 and the K^+ ions. Thus, by small shifts in a few atoms a centrosymmetric structure can be achieved. It is interesting to note that there is not a direct correspondence of equivalent positions in $P2_12_12_1$ and $P2_1/c$. However, the equivalent positions of all three Si atoms in the two space groups duplicate each other. For example, two equivalent positions from S1 and two from Si3 in $P2_1/c$ duplicate the four equivalent positions of Si1 in the orthorhombic space group and so forth. The same is true for the oxygens.

The zirconium and titanium trisilicates are isostructural and contain two types of tunnels that run parallel to the c axis direction (orthorhombic cell). The larger tunnels are circumscribed by 16 Ti−O−Si atoms (eight-membered ring in zeolite notation) and are surrounded by four of the smaller tunnels with six-membered ring openings. The two sets of tunnels are connected by seven-membered rings disposed perpendicularly to the direction of the tunnels. Half the potassium atoms are located in the larger channel and designated as K1 (or

(30) Farrugia, L. J. MISSYM algorithm in program WinGX; University of Glasgow: Glasgow, U.K., 1998.

M1 in general), and the remainder reside in the smaller channel near the seven-membered connecting ring and are designated as K2(M2).

A comparison of K−O bond lengths in the Zr and Ti trisilicate compounds is given in Table 5. Except for K1−O10 and K2−O2, all other K−O interatomic distances are longer in the Zr compound than in the Ti compounds. The difference varies between 0.04 and 0.19 Å The average difference in K−O distances is 0.12 Å for potassium ion, K1, while it is 0.08 Å for K2. Most of the distances in the Ti compound are within the range for reasonable K−O bond lengths (r_{K^+} $r_{O^{2-}} = 2.76$ Å) while in the Zr compound they are on the upper limit for good K−O bonds. It could be for this reason that the Ti compound prefers the K^+ ions in the channels and therefore they are difficult to exchange for Cs^+ ions. On the other hand, due to the enlarged cavity size, the potassium ions could be easily exchanged for Cs^+ ions in the zirconium compound. It may be noted that many of the K−O interatomic lengths observed for the Zr compounds are closer to reasonable Cs−O bond lengths than in the Ti compound. This bond length correspondence may account for the high cesium ion selectivity in the Zr compound. The Ti compound, on the other hand, shows very little selectivity for Cs^+ as only about 10% of the total H^+ of H_3O^+ ions could be exchanged for Cs^+ ions without the use of base (Figure 15).

Our earlier study[16] on exchange of Cs^+ for K^+ in $K_2ZrSi_3O_9 \cdot H_2O$ showed that complete exchange of Cs^+ for K^+ is possible. At a composition level of $K_{0.9}Cs_{1.1}ZrSi_3O_9 \cdot 2H_2O$ the bulk of the Cs^+ is located in the narrower tunnels (M2 site) with most of the K^+ in the larger tunnels. With additional exchange to a cation composition of $K_{0.5}Cs_{1.5}$ all the M2 sites contain Cs^+. However, Cs^+ is too large to fit through the six-membered ring openings into the smaller tunnels where the M2 sites are located. Therefore, the cesium ion must enter the larger tunnels and diffuse into the smaller ones. In the process, the unit cell volume increases from 987 Å^3 for the potassium phase to 1053 Å for the $K_{0.5}Cs_{1.5}ZrSi_3O_9 \cdot H_2O$ phase. The unit cell volumes of the titanium phases I and II are considerably smaller than those of the zirconium phases. Thus, we surmise that Cs^+ can only enter the larger tunnels and cannot diffuse to the M2 site because of the smallness of the volume available. As a result much less Cs^+ is exchanged by the protonated titanium trisilicate.

We have also prepared a series of mixed titanium−zirconium trisilicate phases.[31] A solid solution series was prepared with Zr contents of 25, 50, 63, 75, and 88% Zr. Determination of the corrected selectivity coefficients, K_c, for Cs^+ exchange showed a continuous increase in K_c from the pure Ti phase to the pure Zr phase. This increase is attributed to the corresponding increase in the channel widths as the larger Zr replaces Ti.

With this structural background, we are now in a position to describe the observed ion exchange behavior and selectivities. According to Eisenman[32,33] the exchange process can be broken down into an electrostatic free energy and a hydration free energy. The former effect is equivalent to bringing a gaseous ion from infinity to its position within the tunnel. At the same time, protons are brought from their position within the tunnel to infinity. On the assumption that the ions are unhydrated within the tunnels the hydration effect is just the difference in free energy of the two exchanging ions. In the strong field case, where a high negative charge is concentrated in a few lattice oxygens, Li^+ would be the most preferred of the alkali metal ions because it would form a strong bond with the highly charged oxygen and it has the highest hydration free energy of the group 1 cations or lowest value of ($\Delta G°_{H+} - \Delta G°_{Li}$) hydration. In the weak field case Cs^+ would be expected to be the most preferred ion. The titanium trisilicate is decidedly a weak field exchanger as each oxygen has a negative charge of $^2/_9$ e$^-$. However, Cs^+ is too large to occupy all the exchange sites in the Ti phase, compound I, as shown by its low uptake of 2 mequiv/g. However, for those initial sites the selectivity against protonic forms is high as attested to by the large K_d values in Tables 7 and 8. We also observe that the K_d values for cesium exchange for K^+ in $K_2TiSi_3O_9 \cdot H_2O$ are low. Potassium ions are small enough to occupy all the exchange sites and to form strong bonds with the framework oxygens. Furthermore, the difference in hydration energies between Cs^+ and K^+ is only 12.9 kcal/mol.[34] This is more than compensated by the favorable bonding situation for K^+. Another factor to consider is that the unit cell volume would have to expand to accommodate Cs^+. Therefore, in the titanium trisilicate all the factors favor K^+ selectivity over that of cesium ion.

In the case of alkaline earth cations there is a very sizable increase in the free energies of hydration, in fact more than four times larger than those of the alkali cations.[34] An even larger increase characterizes the first-row transition elements.[35] These increases in $\Delta G°$ of hydration are sufficient to lower the affinity toward these ions drastically. The exclusion of highly hydrated ions is a form of ion sieving. If the bond-breaking bond-making reaction does not supply sufficient energy to effect dehydration of the incoming ion, then it remains too large to diffuse into the solid exchanger.

It is interesting to note that the mineral umbite[36] has the composition $K_2(Zr_{0.8}Ti_{0.2})Si_3O_9 \cdot H_2O$ and is probably isostructural to the compounds described here since it is orthorhombic, space group $P2_12_12_1$ and has similar unit cell dimensions as the potassium zirconium trisilicate. Lin et al.[37] concluded that umbite and $K_2TiSi_3O_9 \cdot H_2O$ were isostructural from the correspondence of their X-ray powder patterns. A mineral analogue of $K_2ZrSi_3O_9 \cdot H_2O$ is also known.[38]

Acknowledgment. We acknowledge with thanks financial support of this study by the U.S. Department

(31) Clearfield, A.; Bortun, A. I.; Bortun, L. N.; Poojary, D. M.; Khainakov, S. A. *J. Mol. Struct.* **1998**, *469*, 207.
(32) Eisenman, G. *Biophys. J. Suppl.* **1962**, 2, 259.
(33) Clearfield, A *Chem. Rev.* **1988**, 88, 125.
(34) Nancollas, G. H. *Intercalations in Electrolyte Solutions*; Elsevier: New York, 1966; p 121.
(35) Figgis, B. N. *Introduction to Ligand Fields*; Wiley Interscience: New York, NY, 1966; p 91.
(36) Henshaw, D. E. *Miner. Mag.* **1955**, *30*, 585.
(37) Lin, Z.; Rocha, J.; Brandao, P.; Ferreira, A.; Esculcas, A. P.; Pedrosa de Jesus, J. D. *J. Phys. Chem. B* **1997**, *101*, 7114.
(38) Ilyukhin, G. D.; Pudovkina, Z. V.; Voronkov, A. A. *Dokl. Akad. Nauk SSSR* **1982**, *257*, 608.

of Energy, Grant No.198567-A-F1 through the Oak Ridge National Laboratory under DOE's Office of Science and Technology's Efficient Separations and Processing Crosscutting Program and Basic Energy Sciences Division of the Department of energy, grant 9600868 with funds supplied by Environmental Management (EMSP). We thank Dr. Robert Taylor of Texas A&M University for assistance with the NMR measurements.

CM990126Z